Laser-induced thermal effects on the optical properties of free-standing porous silicon films

Hideki Koyama[a] and Philippe M. Fauchet
Department of Electrical and Computer Engineering, University of Rochester, Rochester, New York 14627

(Received 17 August 1999; accepted for publication 15 November 1999)

A detailed study of the unique optical properties of free-standing oxidized porous silicon films has been performed. Under continuous-wave laser irradiation, a strongly superlinear light emission and a very large laser-induced absorption are observed. The nonlinear emission is characterized by a sharp intensity increase that is in proportion to at least the eighth power of the excitation intensity. This emission has a broad peak (600–1300 nm), slow time constant ($\geqslant$10 ms), and very low polarization memory ($\leqslant$0.01 near the emission peak). The induced absorption increases linearly with the pump laser intensity and can be as large as several times the linear absorption. The increase in the normalized absorption coefficient is almost independent of the oxidation temperature and emission wavelength, with essentially no polarization dependence. These experimental results are discussed in terms of laser-induced thermal effects. An evaluation of the temperature rise under the laser irradiation is performed both experimentally and theoretically. A remarkably high-temperature rise of $\geqslant$700 °C is estimated for a moderate excitation intensity of 20 W/cm^2. © *2000 American Institute of Physics.* [S0021-8979(00)08104-4]

I. INTRODUCTION

Electrochemical anodization of Si wafers in a HF solution at a moderate current density results in the formation of a porous silicon (PSi) layer.[1] Since the first observation of its visible photoluminescence (PL) (Ref. 2) and electroluminescence,[3] PSi has received great attention as a material for novel Si optoelectronic devices.[4–8] The light emission from PSi is most often attributed to the quantum-size effect[2,9] in Si nanocrystallites. Some recent studies[10,11] have shown that the participation of the surface bond(s) on the Si nanocrystallites is important in the strong red emission from air-exposed PSi. Luminescence mechanisms without invoking the quantum-confinement hypothesis have also been discussed.[12–14]

One of the unique properties of PSi is that a free-standing film can easily be obtained by increasing the current density to the electropolishing regime at the end of the anodization.[15–17] Such free-standing films have been used in characterizing the optical absorption or other properties of PSi without the effect of the Si substrate. In nonlinear transmission experiments,[18–20] the PSi film is often excited with a very high (average) intensity up to several hundred W/cm^2. In most cases, however, little attention has been paid to the possible heating effect of the laser beam.

Recently, we reported the observation of a strongly nonlinear light emission[21] and a very large induced absorption[22] in thermally oxidized free-standing PSi films under continuous-wave laser irradiation. Since both of these phenomena were found to be quenched significantly when the samples were cooled (by attaching the film to a higher-thermal-conductivity material or by blowing air), we suggested a very high-laser-induced temperature rise as a possible origin. Oxidation itself is not responsible for these phenomena, because as-anodized free-standing PSi samples also show the same absorption increase up to the laser intensity at which they are destroyed.[22]

In this article, we report on the results of a detailed study on these two interesting optical phenomena in order to confirm the hypothesis of the heat-induced effect. Estimation of the temperature rise is carried out both experimentally and theoretically.

II. EXPERIMENT

PSi samples were prepared by the anodization of (100) p^+-Si wafers (0.008–0.012 Ω cm) in a solution of 50% HF:ethanol=1:1 at a current density of 100 mA/cm^2 for 2.5 min. At the end of the anodization, the current density was abruptly increased to ~700 mA/cm^2 to lift off the PSi layers. The thickness of these PSi films is about 12 μm. Thermal oxidation was then carried out in dry O_2 at 800–1000 °C for 10 min.

Light-emission spectra were measured under excitation with a multiline (457.9–514.5 nm) Ar^+ laser beam focused to a spot of ~1 mm in diameter using a cooled Ge detector with a lock-in technique. The measured spectra were then corrected for the apparatus response. In some samples, we evaluated the degree of polarization memory (PM).[23,24] In the PM measurements, the PSi samples were excited by a linearly polarized 514.5 nm line of the Ar^+ laser. The excitation laser beam was incident normally to the sample surface after passing through a polarization rotator (half-wave plate). The emission was collected through an analyzer placed at a small angle off the normal direction. The degree of PM is defined by $P=(I_{\parallel}-I_{\perp})/(I_{\parallel}+I_{\perp})$, where $I_{\parallel}$ and $I_{\perp}$ are the intensities of the emission components polarized par-

[a]Present address: Hyogo University of Teacher Education, Yashiro, Hyogo 673-1494, Japan. Electronic mail: koyama@life.hyogo-u.ac.jp

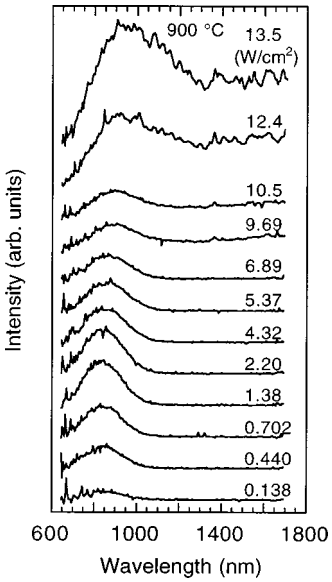

FIG. 1. Emission spectra of a free-standing PSi sample (oxidized at 900 °C) at different excitation intensities.

allel and perpendicular, respectively, to the polarization direction of the excitation light. In order to cancel out the polarization-dependent response of the monochromator, $I_{\parallel}$ and $I_{\perp}$ were measured by changing the polarization direction of the excitation light by 90° while keeping the analyzer fixed. A Si diode array detector and a film analyzer ($\leqslant$800 nm) were used for the measurements of PM.

The optical absorption measurements were carried out using a pump–probe technique. The pump beam was a multiline Ar^+ laser with a spot of ~1 mm in diameter. The probe beam was either a 632.8 nm He–Ne laser or the multiline Ar^+ laser. The spot size of the probe beam was slightly less than that of the pump beam.

III. RESULTS AND DISCUSSION

A. Superlinear light emission

Figure 1 shows the emission spectra measured at different excitation intensities for a PSi film oxidized at 900 °C. The emission intensities at six different emission wavelengths are plotted in Fig. 2 as a function of the excitation intensity. At low excitation intensities ($\leqslant$2 W/cm^2), the PL peaks at ~850 nm and increases linearly with excitation intensity, which is the usual behavior for these samples. For increasing excitation intensities, the emission intensity first decreases, followed by the appearance of a strongly nonlinear emission that is shifted to the red and has a very broad spectral width. The intensity of this strong emission (I_{em}) can be expressed as a function of the excitation intensity (I_{ex}) by the power law $I_{em} \propto I_{ex}^n$ with $n \geqslant 8$.

As mentioned above, our preliminary experimental results[21] suggested a heat-induced mechanism as the origin of this phenomenon. Indeed, its spectral features are very similar to those of the thermal radiation from bulk crystalline Si.[25] In order to confirm this, the excitation laser beam was chopped at different frequencies to estimate the response time of this emission. Figures 3(a) and 3(b) show the

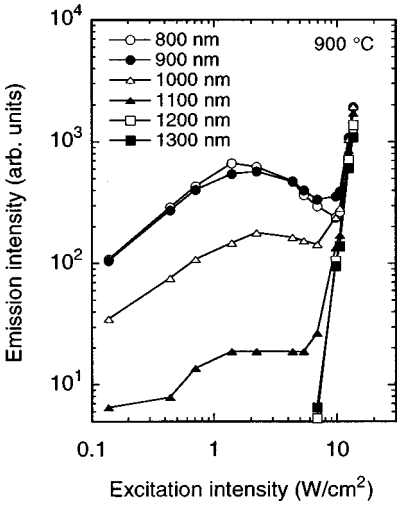

FIG. 2. Emission intensity at different wavelengths as a function of the excitation intensity for the sample of Fig. 1.

chopping-frequency dependence of the emission spectra for PSi samples oxidized at 900 and 800 °C, respectively. The major difference between these two samples is that the sample oxidized at 900 °C exhibits significant linear PL at

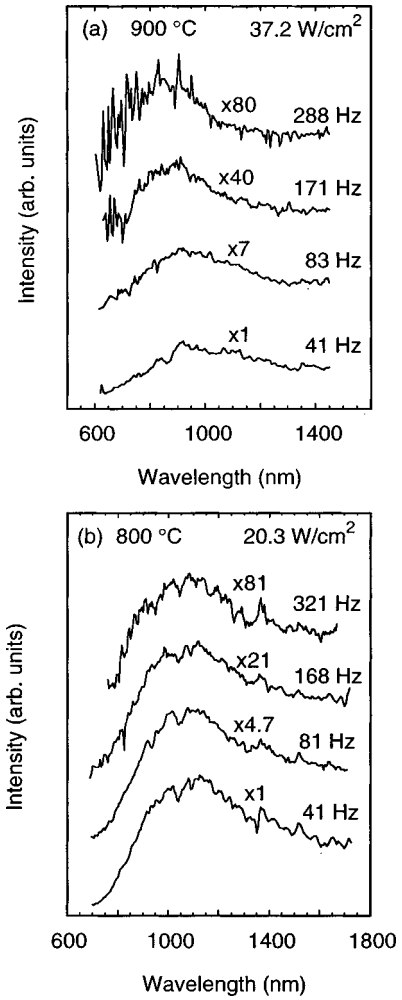

FIG. 3. Chopping-frequency dependence of emission spectra in free-standing PSi samples oxidized at 900 °C (a) and 800 °C (b).

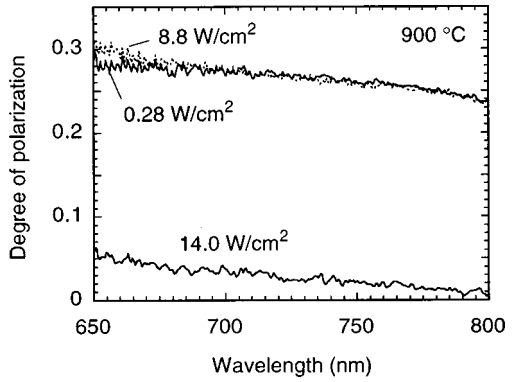

FIG. 4. Degree of PM as a function of the emission wavelength at different excitation intensities for the sample of Fig. 1.

low excitation intensities, as shown in Fig. 1. The sample oxidized at 800 °C, in contrast, exhibits very weak linear PL compared to the intensity of the strong superlinear emission. As seen from Fig. 3(a), the emission spectra for the sample oxidized at 900 °C show a blueshift with increasing chopping frequencies. This blueshift is due to the appearance of the linear PL that has been overwhelmed by the strong superlinear emission at low frequencies. No significant shift in emission spectra is observed in the sample oxidized at 800 °C, as shown in Fig. 3(b). The redshift in Fig. 3(a), therefore, implies that the time constant of the superlinear emission is much longer than that of the linear PL (normally ~100 μs).[26] We find that the response time of the superlinear emission is of the order of 10 ms or longer, since the emission intensity decreases significantly with decreasing chopping frequencies (note that the spectra in Fig. 3 are magnified as indicated). The relatively long time constant is suggestive of a thermally induced mechanism.

The hypothesis of a heat-related origin is further supported by the experimental results of PM. Figure 4 shows the degree of PM for three different excitation intensities as a function of the emission wavelength. When the excitation intensity is lower than the threshold of the superlinear emission (~10 W/cm^2), we observe a large degree of PM that is almost independent of the excitation intensity. The degree of PM, however, decreases drastically when the excitation intensity is increased and the superlinear emission dominates the spectrum. Polarization memory in PL is thought to occur as a result of the radiative recombination of photoexcited excitons localized at anisotropic energy states.[23,24] The almost complete quenching of the PM, therefore, implies that the carriers have moved away from original states by thermal excitation, or that the carriers are excited thermally instead of by optical excitation.

According to Daub and Würfel,[27] the emission intensity $I(\lambda)$ at a wavelength λ resulting from the band-to-band radiative recombination at a temperature T is given by

$$I(\lambda)=A\frac{a(\lambda)}{\lambda^5}\exp\left(-\frac{hc/\lambda-\mu}{kT}\right)\left[\exp\left(\frac{hc/\lambda-\mu}{kT}\right)\gg 1\right], \quad (1)$$

where A is a constant, $a(\lambda)$ is the absorptivity, h is Planck's constant, c is the speed of light, and k is Boltzmann's constant. μ is the difference between the electron and hole quasi-Fermi energies. When $\mu=0$, Eq. (1) reduces to the thermal radiation formula for temperature T. If the temperature dependence of $a(\lambda)$ and μ are small, $I(\lambda)$ is thermally activated with an activation energy $\Delta E=hc/\lambda-\mu$. In our results (Fig. 1), the major part of the superlinear emission has a photon energy $hc/\lambda\geqslant 1$ eV. Thus, unless μ is very large, $I(\lambda)$ has an activation energy large enough to show a very sharp increase with increasing the excitation light intensity (the increase in T is almost proportional to the excitation intensity as shown below). Indeed, satisfactory single-exponential relationships can be obtained if the emission intensity data shown in Fig. 2 are replotted as a function of inverse temperature (the temperature will be estimated below). These relationships give an activation energy of ~1 eV, which verifies the validity of a low μ. This low μ is due to the prevalence of relatively fast, nonradiative transitions as indicated by the very low PL efficiency of the sample ($<10^{-4}$). A detailed analysis of the emission intensity based on Eq. (1), however, should take into account the temperature dependence in both $a(\lambda)$ and μ.

It should be noted that the emission is not pure thermal radiation[28] and there is a contribution from PL unless μ is absolutely zero. The ratio of the total emission intensity to the thermal radiation component is given by $\exp(\mu/kT)$, independent of the emission wavelength (this means that the PL has the same spectral features as those of the thermal radiation). Thus, even if μ is only several times as large as kT, the emission is dominated by PL. A possible physical origin for the superlinear increase in PL intensity is the thermal reexcitation of trapped carriers.[21] A significant amount of such trapped carriers are suggested to be present in nonluminescent Si nanocrystallites under photoexcitation.[29]

B. Induced absorption

In Fig. 5, we show the normalized induced absorption coefficient $\Delta\alpha/\alpha_0$ (α_0: linear absorption coefficient) for two different probe wavelengths as a function of the pump laser intensity. In either case, $\Delta\alpha/\alpha_0$ increases linearly with increasing pump intensities, reaching a value greater than unity at a pump intensity of ~10 W/cm^2. $\Delta\alpha/\alpha_0$ is almost independent of the sample oxidation temperature, in spite of the large dispersion in α_0, as shown in Fig. 6. Even as-anodized samples ($\alpha_0=1180\,\mathrm{cm}^{-1}$) follow the same relationship.

There is enough evidence that the large laser-induced absorption increase is due to thermal effects as opposed to the absorption by excited carriers. First, the induced absorption decreases precipitously when the sample is attached to materials with a higher thermal conductivity (e.g., sapphire).[22] Second, the fact that $\Delta\alpha/\alpha_0$ does not depend on the oxidation temperature suggests a bulk effect rather than mechanisms involving quantum-confined or surface states, the latter of which have been proposed as responsible for the large induced absorption in PSi.[19] Third, the nearly identical values of $\Delta\alpha/\alpha_0$ for different probe wavelengths are a characteristic of thermally induced absorption.[30,31]

We now present another piece of evidence from the measurement of the polarization dependence. Figure 7 shows the induced absorption coefficient $\Delta\alpha$ for two different

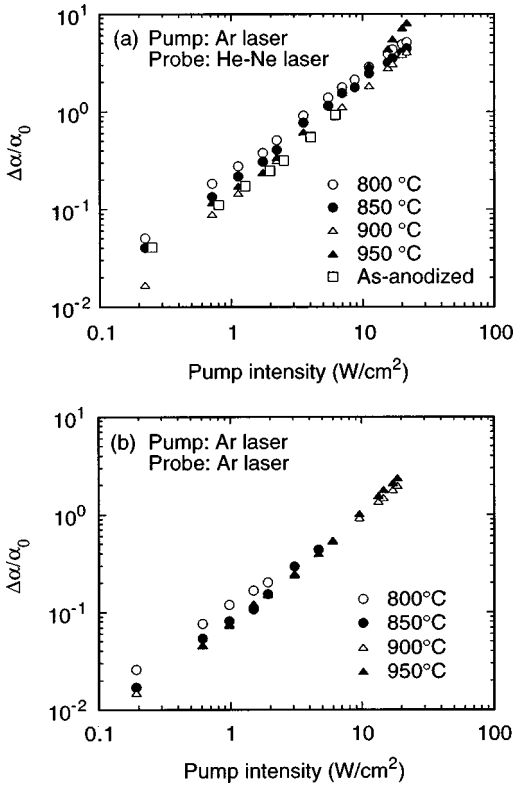

FIG. 5. Normalized induced absorption coefficient in different PSi samples as a function of the pump laser intensity. The induced absorption was measured with a multiline (457.9–514.5 nm) Ar^+ laser pump beam and a 632.8 nm He–Ne laser (a) or a multiline Ar^+ laser (b) probe beam.

samples measured under two different polarization conditions, i.e., $\mathbf{E}_{\text{pump}} \| \mathbf{E}_{\text{probe}}$ and $\mathbf{E}_{\text{pump}} \perp \mathbf{E}_{\text{probe}}$, where $\mathbf{E}_{\text{pump}}$ and $\mathbf{E}_{\text{probe}}$ are the electric-field vectors of the pump and probe light, respectively. The experimental results show no significant polarization dependence in $\Delta\alpha$, in spite of a large PM in the light emission, as shown in Fig. 4. This suggests that large, bulk-like nonluminescent Si regions are mainly responsible for the large $\Delta\alpha$ through the thermal effect.

In some samples oxidized at 1000 °C, we observed a significant increase in transparency, i.e., bleaching, with increasing pump intensities. However, the tendency was reversed when the incident angle of the probe beam was changed slightly, as shown in Fig. 8. This means that the real part of the refractive index also changes in these PSi films as a result of heating by the pump laser beam. The dependence of the transmittance on the incidence angle is due to a change in the interference conditions through a change in the refractive index. The bleaching was not observed in samples oxidized at 950 °C or below because of the lack of importance of the interference effect in these low-transmission samples.

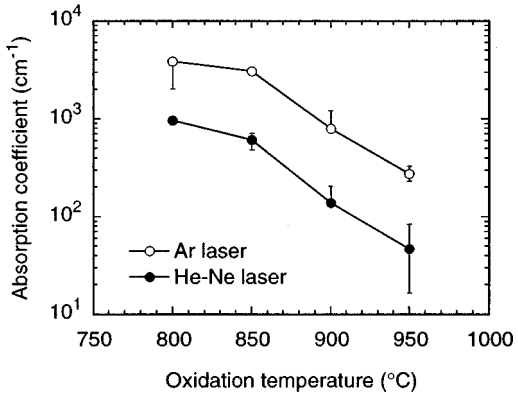

FIG. 6. Linear absorption coefficient for two different laser beams (multiline Ar^+ laser and 632.8 nm He–Ne laser) as a function of the oxidation temperature.

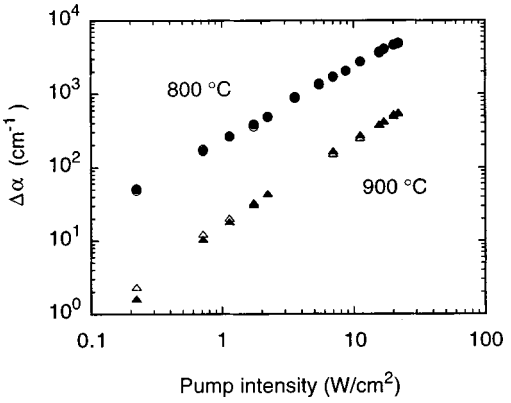

FIG. 7. Induced absorption coefficient in two PSi samples measured under different polarization configurations: open and closed symbols show the data measured with the probe beam (632.8 nm) polarized parallel and perpendicular, respectively, to the polarization direction of the pump beam.

C. Evaluation of the temperature rise

1. Raman scattering

Raman scattering spectra were obtained by exciting with the 514.5 nm line from an Ar^+ laser. Figure 9 shows the measured spectra for on-substrate (a) and free-standing (b) samples, both of which have been prepared by thermal oxidation at 900 °C. A remarkable peak shift with significant spectral broadening is observed in the free-standing sample with increasing excitation intensities, suggesting a large temperature rise due to laser heating. In contrast, the on-substrate sample shows little excitation-intensity dependence. The peak shift as a function of the excitation intensity is plotted in Fig. 10.

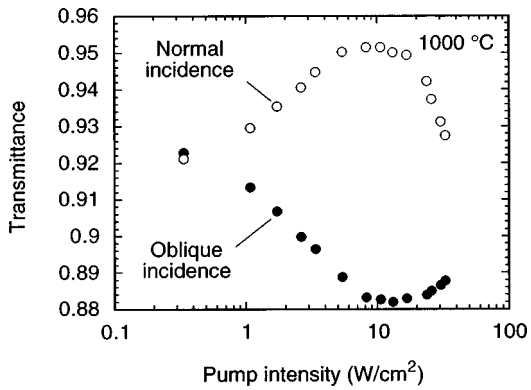

FIG. 8. Pump-intensity dependence of transmittance in a free-standing PSi sample oxidized at 1000 °C. The open and closed symbols show the data measured with different incident angles of the probe beam (632.8 nm).

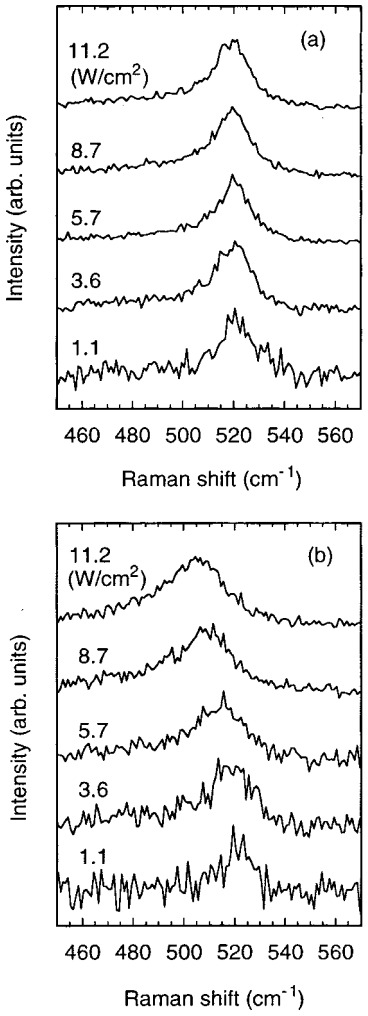

FIG. 9. Excitation-intensity dependence of Raman scattering spectra in on-substrate (a) and free-standing (b) PSi samples oxidized at 900 °C.

We assume that the Raman spectra reflect the properties of large, bulk-like crystalline Si regions and not those of nanosize Si crystallites. This is a reasonable assumption because the peak position in the lower-excitation-intensity limit approaches that of the bulk crystalline Si at room temperature (522 cm^{-1}). Since the temperature dependence of the Raman scattering peak in crystalline Si is well established,[32]

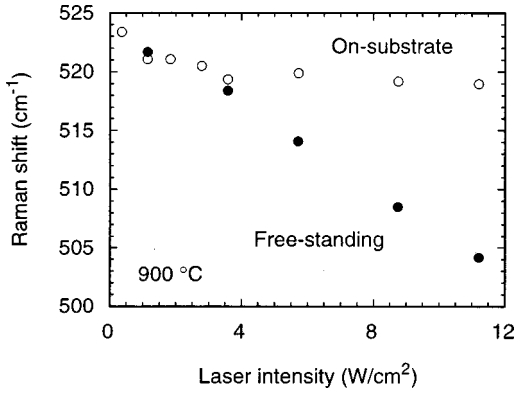

FIG. 10. Raman shift in on-substrate (open circles) and free-standing (closed circles) PSi samples as a function of the excitation laser intensity.

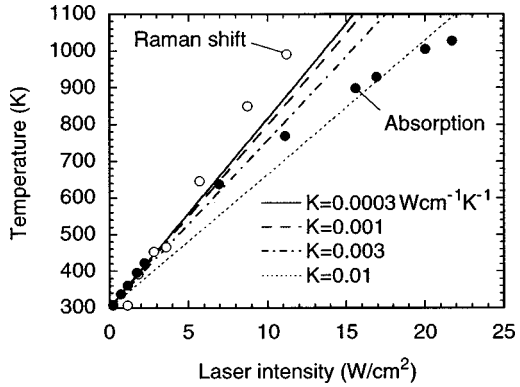

FIG. 11. Results of the temperature estimation in the PSi sample oxidized at 900 °C. The open and closed circles show the values obtained from the Raman shift and the induced absorption coefficient (at 632.8 nm), respectively. Straight lines are the results of the theoretical calculation performed for four different thermal conductivities.

we can estimate the temperature in our PSi samples from the data in Fig. 10. The result for the free-standing sample is plotted in Fig. 11 by the open circles. The estimated temperature shows a linear increase with increasing excitation intensities, reaching a very high value of ~1000 K at 11 W/cm^2.

2. Absorption

Jellison and Modine[30] have derived an empirical formula for the temperature-dependent absorption coefficient of bulk crystalline Si. According to the experimental results shown in Fig. 5, oxidation does not change the normalized absorption coefficient of PSi significantly. Therefore, we assume that the same formula can be used to describe the temperature dependence of $\Delta\alpha/\alpha_0$ in our oxidized PSi samples:

$$\frac{\Delta\alpha}{\alpha_0}=\exp\left(\frac{T-T_0}{T_A}\right)-1, \tag{2}$$

where T_0 is the ambient temperature, and T_A is a constant that depends on the wavelength ($T_A=447$ K at 632.8 nm). The values of temperature calculated from the data in Fig. 5(a) using Eq. (2) are plotted in Fig. 11 by closed circles. These temperatures also show very high values exceeding 1000 K at 22 W/cm^2.

3. Theoretical calculation

The calculation presented below is based on the approach used by Lax[33] for the analysis of the temperature rise in laser-irradiated semi-infinite media. We extended this model to the system of an absorbing film (PSi) sandwiched between two semi-infinite nonabsorbing media (air). A similar extension of Lax's model has been performed by Tang and Herman[34] for the case of an absorbing film on a semi-infinite transparent substrate. The major difference is that in our model there is a heat flow from the film into air (the thermal conductivity of air is $K_0=2.6\times10^{-4}$ W cm^{-1} K^{-1}). Therefore, we solved the steady-state heat flow equation in three regions (air/film/air) with proper boundary conditions (continuum of temperature and heat flux)[35] at the two interfaces. Nonlinear heat dissipation mechanisms such as natural

convection and radiation were not considered for simplicity. The result for the temperature rise ΔT at the center of the Gaussian laser beam (peak intensity I_0 and beam waist radius w) on the front surface of the film (thickness d, absorption coefficient α, and thermal conductivity K) is

$$\Delta T = B\int_0^{\infty} \frac{M(\xi)F(\xi)}{W^2-\xi^2}\,d\xi,$$

where

$$M(\xi) = \frac{K}{K-K_0}\left[\frac{2A_2(\xi)}{A_1(\xi)} - W - \xi\right],$$

and

$$A_1(\xi) = (K+K_0)^2 e^{\xi D} - (K-K_0)^2 e^{-\xi D},$$

$$A_2(\xi) = (K+K_0)(KW+K_0\xi)e^{\xi D} - (K-K_0)(KW-K_0\xi)e^{-WD}.$$

The normalized variables $W=\alpha w$ and $D=d/w$ have been used.[33,34] Also,

$$F(\xi) = (1/2)\exp(-\xi^2/4),$$

$$B = \alpha I_0 w^2/K.$$

As expected, the temperature rise ΔT is proportional to the incident laser intensity I_0. It should be noted that neglecting the heat flow from the film surfaces results in an infinite temperature rise [since $A_1(0)=0$ when $K_0=0$] regardless of the values of the thermal conductivity and the film thickness.

The calculated temperatures for several different thermal conductivities are shown in Fig. 11 by straight lines. It can be seen that the experimental temperature values obtained from the absorption data at low excitation intensities ($\leqslant 10$ W/cm^2) are well reproduced with a thermal conductivity lower than $3\times10^{-3}\,\mathrm{W\,cm^{-1}\,K^{-1}}$. This very low thermal conductivity is consistent with the measured values in as-anodized PSi reported by several groups.[36,37] We have already shown in Fig. 5(a) that oxidized PSi samples have similar thermal properties to those of as-anodized ones.

At higher excitation intensities, the temperatures obtained from the absorption measurements depart from the linear relationship and tend to saturate with increasing excitation intensities. This can be explained by the effect of natural convection and/or thermal radiation, both of which become significant at high temperatures.[35] Also, the increase of the thermal conductivity at high temperatures[36] should contribute to the sublinear increase of the temperature rise. The temperature obtained from the Raman scattering measurements show slightly higher values than those calculated with any thermal conductivity $K>K_0$. This suggests that compressive stress[38] due to localized heating is also responsible for the large shift in the Raman spectra.

IV. CONCLUSION

We have presented a detailed investigation of the unique emission and absorption properties of free-standing PSi films observed under excitation by a moderate-intensity ($\leqslant 20$ W/cm^2), continuous-wave laser beam. The superlinear light emission is characterized by a remarkably sharp increase of intensity with increasing excitation intensities. This emission exhibits a very broad peak ($600<\lambda<1300$ nm), a slow response time (>10 ms), and a low polarization memory (<0.01 near the emission peak). The induced absorption coefficient shows a linear increase with increasing excitation laser intensities. The normalized induced absorption coefficient $\Delta\alpha/\alpha_0$ is almost independent of the sample oxidation temperature and the emission wavelength. No significant polarization dependence has been observed. All of these results are consistent with the hypothesis of the laser-induced thermal effect. This is further supported by the experimental (by Raman scattering and absorption measurements) and theoretical temperature estimation, which has resulted in a very high-temperature rise of $\geqslant 700\,^{\circ}$C for a moderate excitation intensity of 20 W/cm^2.

ACKNOWLEDGMENTS

The authors thank L. Tsybeskov and H. A. Lopez for technical assistance. This work was supported by the Army Research Office.

[1] A. Uhlir, Jr., Bell Syst. Tech. J. **35**, 333 (1956).
[2] L. T. Canham, Appl. Phys. Lett. **57**, 1046 (1990).
[3] N. Koshida and H. Koyama, Appl. Phys. Lett. **60**, 347 (1992).
[4] L. Pavesi, R. Guardini, and C. Mazzoleni, Solid State Commun. **97**, 1051 (1996).
[5] A. Loni, L. T. Canham, M. G. Berger, R. A. Fischer, H. Munder, H. Luth, H. F. Arrand, and T. M. Benson, Thin Solid Films **276**, 143 (1996).
[6] K. D. Hirschman, L. Tsybeskov, S. P. Duttagupta, and P. M. Fauchet, Nature (London) **384**, 338 (1996).
[7] M. Araki, H. Koyama, and N. Koshida, Appl. Phys. Lett. **69**, 2956 (1996).
[8] S. Chan and P. M. Fauchet, Appl. Phys. Lett. **75**, 274 (1999).
[9] V. Lehmann and U. Gösele, Appl. Phys. Lett. **58**, 856 (1991).
[10] H. Koyama, N. Shima, and N. Koshida, Phys. Rev. B **53**, R13291 (1996).
[11] M. V. Wolkin, J. Jorne, P. M. Fauchet, G. Allan, and C. Delerue, Phys. Rev. Lett. **82**, 197 (1999).
[12] P. Deak, M. Rosenbauer, M. Stutzmann, J. Weber, and M. S. Brandt, Phys. Rev. Lett. **69**, 2531 (1992).
[13] S. M. Prokes and O. J. Glembocki, Phys. Rev. B **49**, 2238 (1994).
[14] J. L. Gole and D. A. Dixon, Phys. Rev. B **57**, 12002 (1998).
[15] M. I. J. Beale, J. D. Benjamin, M. J. Uren, N. G. Chew, and A. G. Cullis, J. Cryst. Growth **73**, 622 (1985).
[16] H. Koyama, M. Araki, Y. Yamamoto, and N. Koshida, Jpn. J. Appl. Phys., Part 1 **30**, 3606 (1991).
[17] J. von Behren, L. Tsybeskov, and P. M. Fauchet, Appl. Phys. Lett. **66**, 1662 (1995).
[18] T. Matsumoto, N. Hasegawa, T. Tamaki, K. Ueda, T. Futagi, H. Mimura, and Y. Kanemitsu, Jpn. J. Appl. Phys., Part 2 **33**, L35 (1994).
[19] T. Matsumoto, M. Daimon, H. Mimura, Y. Kanemitsu, and N. Koshida, J. Electrochem. Soc. **142**, 3523 (1995).
[20] V. Klimov, D. McBranch, and V. Karavanskii, Phys. Rev. B **52**, R16989 (1995).
[21] H. Koyama, L. Tsybeskov, and P. M. Fauchet, J. Lumin. **80**, 99 (1999).
[22] H. Koyama and P. M. Fauchet, Appl. Phys. Lett. **73**, 3259 (1998).
[23] H. Koyama and N. Koshida, Phys. Rev. B **52**, 2649 (1995).
[24] D. Kovalev, M. Ben Chorin, J. Diener, F. Koch, Al. L. Efros, M. Rosen, N. A. Gippius, and S. G. Tikhodeev, Appl. Phys. Lett. **67**, 1585 (1995).
[25] P. J. Timans, J. Appl. Phys. **74**, 6353 (1993).
[26] A. Takazawa, T. Tamura, and M. Yamada, J. Appl. Phys. **75**, 2489 (1994).
[27] P. Würfel, J. Chem. Phys. **15**, 3967 (1982); E. Daub and P. Würfel, Phys. Rev. Lett. **74**, 1020 (1995); E. Daub and P. Würfel, J. Appl. Phys. **80**, 5325 (1996).
[28] J. Costa, P. Roura, J. R. Morante, and E. Bertran, J. Appl. Phys. **83**, 7879 (1998).

[29] C. Delerue, G. Allan, and M. Lannoo, Phys. Rev. B **48**, 11024 (1993).
[30] G. E. Jellison, Jr. and F. A. Modine, Appl. Phys. Lett. **41**, 180 (1982).
[31] D. Kovalev, G. Polisski, M. Ben-Chorin, J. Diener, and F. Koch, J. Appl. Phys. **80**, 5978 (1996).
[32] M. Balkanski, R. F. Wallis, and E. Haro, Phys. Rev. B **28**, 1928 (1983).
[33] M. Lax, J. Appl. Phys. **48**, 3919 (1977).
[34] H. Tang and I. P. Herman, J. Vac. Sci. Technol. A **8**, 1608 (1990).
[35] H. S. Carslaw and J. C. Jaeger, *Conduction of Heat in Solids*, 2nd ed. (Clarendon, Oxford, 1986).
[36] G. Gesele, J. Linsmeier, V. Drach, J. Fricke, and R. Arens-Fischer, J. Phys. D **30**, 2911 (1997).
[37] A. N. Obraztsov, H. Okushi, H. Watanabe, and V. Yu. Timoshenko, Phys. Status Solidi B **203**, 565 (1997).
[38] B. Dietrich, E. Bugiel, H. J. Osten, and P. Zaumscil, J. Appl. Phys. **74**, 7223 (1993).